



ELSEVIER

Available online at www.sciencedirect.com

SCIENCE @ DIRECT®

Journal of Sound and Vibration 284 (2005) 825–849

JOURNAL OF
SOUND AND
VIBRATION

www.elsevier.com/locate/jsvi

Torsional finite elements and nonlinear numerical modelling in vehicle powertrain dynamics

A.R. Crowther*, N. Zhang

Faculty of Engineering, University of Technology, Sydney, P.O. Box 123, Broadway 2007, Sydney, Australia

Received 5 February 2004; received in revised form 15 April 2004; accepted 19 July 2004

Available online 9 December 2004

Abstract

Torsional finite elements for direct, branched and grounded (boundary) connections and geared connections with rigid or elastic tooth mesh are presented. The use of these elements for developing dynamic models of various passenger vehicle powertrains is illustrated and discussed. A six-degree-of-freedom dynamic model for clutch engagement is used to investigate the effect of low-frequency transients on clutch engagement stick–slip and gear backlash in powertrains. Results for free vibration analysis and transient vibration numerical simulations are presented. Attention is paid to the algorithms used in the piecewise nonlinear transient analysis and the method of numerical simulation. The methodology is thoroughly detailed and is discussed for application to higher degree-of-freedom powertrain models.

© 2004 Elsevier Ltd. All rights reserved.

1. Introduction

Powertrain systems, such as in vehicles and ships, can be modelled as torsional elastic systems. These models are used by design engineers for investigating and refining vibration inherent in the powertrain. The powertrain components, engine, gearing, couplings, clutches, etc., can be complex to model. Basic models start with linear-lumped spring–mass systems of equations of motion [1] and improve with additional detail for the dynamics of various components.

*Corresponding author. Fax: +61 2 9514 3147.

E-mail address: crowther@eng.uts.edu.au (A.R. Crowther).

The inertia distribution of vehicle powertrains is light at the engine side and heavy at the wheel, where the vehicle mass is coupled with the torsional system. Torsional stiffness is high in the crankshaft and short gear shafts and low for propeller, drive and some transmission shafts. The shafts exhibit small hysteresis. Piston friction and bearing friction provide small damping and tire hysteresis and fluid couplings provide large damping.

Linearised lumped mass modelling can be used to estimate the natural frequencies of the system. Dynamic systems can be described with torsional finite elements and assembled [1–3]. The models can be used to reduce resonance by designing natural frequencies away from engine harmonics. Commonly, automatic transmission equipped powertrains have torque converter lock-up damper clutches with high hysteresis and single or multistage stiffness, in designing these clutches, stiffness and hysteresis parameter sensitivity analysis can be used to reduce resonance [4–6]. Often this is presented as Campbell plot [4,5]. Stiffness variation in other shafting can be similarly analysed [7]. Some models use distributed mass elements for long shafts with significant mass, such as the propeller or main drive shaft [8], with these elements integrated into a lumped–distributed mass system. Solutions for dynamic models can be found for transient vibration from tip-in engine torque, gear shifts, etc. [4,6,7]. The most commonly investigated transient is the lowest global mode of the torsional system, denoted the shuffle mode (2–10 Hz). It is largely dependent on engine/flywheel inertia, drive shaft stiffness and overall gear ratio.

Models can be improved with addition of the nonlinear phenomena and solutions found numerically for transient dynamics. The various components of the powertrain bring complexity and are nonlinear; the engine can be modelled or measured for combustion torque, the torque converter for transfer torque, bands and clutch for friction characteristics, judder and stick–slip, hydraulics for pressure, gear dynamics for gear shifts, gear meshing for backlash and transmission error, tires for damping, stiffness and slip and then the associated systems—electrical, control, chassis and suspension. Published research for powertrain torsional vibration generally has a focus on dynamic modelling, results and experiments. Not often is the simulation methodology extensively detailed.

Judder is a friction induced vibration between masses with sliding contact. Judder in automotive clutches has been a focus of previous research in both manual and automatic transmissions. It has long been attributed to an increasing friction coefficient with decreasing slipping velocity, dubbed as a negative friction gradient, and is known to reduce with system damping [9,10]. Wet clutch and slipping clutch design calls for the correct combination of friction material and automatic transmission fluid (ATF) to produce a continuously positively sloped friction curve. This helps prevent driveline torsional oscillations excited by clutch judder.

Stick–slip is the nonlinear intermittent sliding and stichon (sticking) at a contact surface. It is a phenomenon with dependence on friction characteristics, system dynamics and external tangential and normal forcing [11]. Most studies concentrate on systems with the sliding interface between one moving and one stationary surface or between one moving and a substrate moving at a predetermined velocity. A great deal of analytical work has been published for various systems [11–14]. In automotive clutches the sliding interface is between two masses with undetermined velocities in a nonlinear non-autonomous system, thus investigation using numerical methods is appropriate. Review and investigation into judder and stick–slip is given in Ref. [15].

Geared systems require clearance between mating gears for smooth operation. The clearance is termed lash and the mating gears must separate across the lash when their relative directions of

rotation change. The mating gears can be modelled with a mesh stiffness which is nonlinear [16]. It is set as zero across the lash zone. ‘Clonk’ is a term used in the automotive industry for the noise produced from impacting gears and splines during torque reversal [17]. Transient dynamics from engine tip/in, gear shifts, etc. can produce a torque reversal (shuffle) thereby inducing clonk. Refs. [6,18] show the relationship between clonk and shuffle, multiple torque reversals were found to cause multiple impacts.

In Ref. [2] torsional vibrations were studied in a vehicle powertrain with a four cylinder engine and manual transmission under steady state and transient operating conditions. A torsional finite element model was developed including gear backlash and a multi-staged nonlinear clutch with dry friction. The lash was used between each gear in a manual transmission and between the differential pinion and ring. They used a lumped parameter approach for the powertrain and linearised the nonlinear elements for determining natural frequencies, mode shapes and steady-state behaviour. The authors included stiffness for the input and output clutch shaft, gear teeth and shafts, drive shafts and wheels. A damping model value of 6% was used, purported to be deduced from experimental results. They developed an experimental test rig that simulated engine harmonics by use of the varying velocity of a Hooke’s joint. Simulations and results from the rig and vehicle tests were compared. The work focused on the torsional phenomena of idle gear rattle, drive rattle, surging and boom.

In Ref. [17] clonk for higher frequency modes was investigated with a test rig and by modal analysis via finite element models of driveshaft pieces. The test rig was a light diesel truck powertrain fitted with a manual transmission. It included all the components from the flywheel to the wheels, thus including all lash in the system. Accelerometers were mounted in locations such as the final drive, shafting and transmission. The recorded tangential acceleration was converted into angular components. Microphones were placed at the transmission and rear axle. They used a shock impulse to excite high-frequency modes and lash impacts. The impulse was ramped up to 150 N m of torque at the flywheel in 80 ms. The driveshaft transient response had a 1–2 ms impact and a 50 ms decay transient. The authors also developed an FE model for a two-piece hollow driveshaft. They found significant frequencies at 1–5 Hz.

In Ref. [19] a model was developed for investigating low-frequency torsional vibration in vehicle driveline systems with manual transmissions. They modelled the powertrain with lumped masses at the flywheel, transmission and final drive, the driveline masses were reduced by gear ratios to an equivalent system. The tires were assumed to be fixed to the ground. Included in the model were the nonlinear effects of backlash, clutch spring stiffness, coulomb friction and the constant velocity joint. The model was used to investigate shuffle. The test rig detailed in Ref. [17] was used to measure acceleration time histories during engine tip-out with accelerometers at nine locations. They found that the transmission flange had the highest response for shuffle with amplitude maximum at 3.06 Hz. With both a discrete Fourier transform of the transfer matrix formulation and from Simulink simulations they found the shuffle natural frequency at 3.34 Hz. This was a reasonably close comparison. Part of their research was on clonk. They commented on the findings of previous authors—that there was a backlash threshold above which backlash increased the shuffle response, below which backlash had no affect on the shuffle response so that only reducing lash would not improve clonk. Their research was further developed [7] with the model modified to use distributed parameter modelling for the propeller shafts and lumped parameters for rest of powertrain. The model was a partially lumped-partially distributed

(DLMT) system as opposed to the original lumped system (LLMT). They noted that ‘the noise (clonk) is either attenuated through hollow driveline pieces, sometimes referred to as the rear clonk, or radiated in the acoustic cavity formed by the clutch bell housing’. This is why the propeller shaft should be modelled as a distributed system—to include its high-frequency contribution to the natural modes. Gearbox backlash was set at 0.04 rad. Simulations were run using MATLAB and Simulink. An impulse torque of 150 N m was applied to the flywheel and the angular velocities and accelerations recorded for the gearbox and final drive. The LLMT gave similar results to DLMT with no backlash thus for the linear system either are acceptable. With lash included the results for the DMLT model had additional high frequency while the results for the LLMT did not. The DLMT model picked up the attenuation of clonk by the propeller shaft.

In Ref. [20] clonk was investigated in the manual transmission of a vehicle powertrain. They developed a dynamic model with eight degrees of freedom, six for the transmission and one each for flywheel and final drive. Included were input, engine and gear stiffness, the latter treated as nonlinear with lash. An experiment was conducted where a powertrain test rig, grounded at the tires, was preloaded at the engine end with 100 N m of torque and released. Angular acceleration traces were taken from the test rig on flywheel, gears and final drive. Numerical simulations were performed with initial preload as per the experiment. The comparison of results presented showed good correlation for torque reversal at around 80 Hz. High-frequency transients from the resulting impacts were seen with rougher correlation. In the final drive the impact transient and decay was around 10 ms.

In this paper torsional finite elements for direct, geared, branched, grounded and gear (rigid and elastic tooth mesh) elements are described. Dynamic models used to represent torsional dynamics of automotive powertrain systems are presented (manual, automatic and CVT) and the method of assembly using finite elements is outlined. One dynamic model is tailored to include the nonlinear dynamics of clutch engagement and gear lash. The model is used for free vibration analysis and for numerical simulations for a typical clutch engagement. Typical vehicle parameters are used. The simulation demonstrates stick–slip and clonk from shuffle response. The focus is on methodology, the algorithms and programming methodology are described in detail. The technique is demonstrated for easy application to detailed powertrain models—such as those that include automatic transmission gear shifting with multi-degree-of-freedom planetary gear and final drive dynamics and clearances.

2. Torsional finite elements

Finite elements are used to represent local coordinates, their inertias and their coupling within global dynamic systems. These elements can then be used to develop a global system of equations of motion via simple matrix assembly. Fig. 1 provides model schematics for five dynamic systems with lumped inertias and connecting damping and stiffness. The five schematics are examples for *direct*, *geared—rigid and elastic mesh*, *branched and grounded* systems. Stiffness and damping parameters are torsional except for the geared connection with elastic mesh where the stiffness parameter represents tooth stiffness normal to the plane of contact. For each system the required torsional finite elements are outlined. The derivation for each element type is not provided as it is

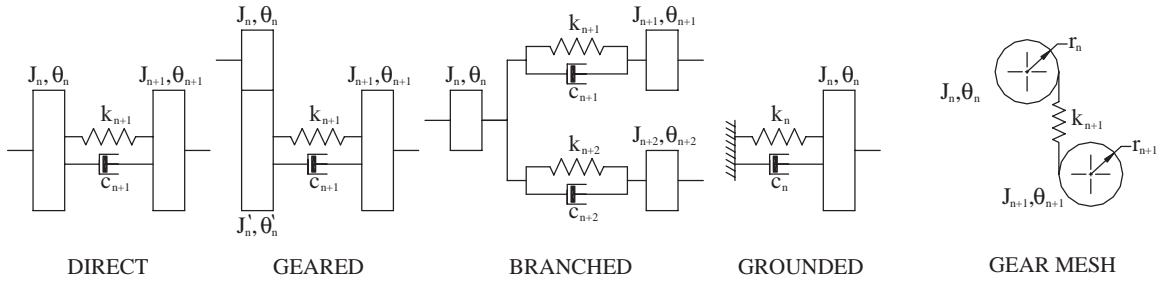


Fig. 1. Model schematics.

elementary. For each system the inertia, stiffness and damping matrices and local coordinate vector are:

Direct:

$$\mathbf{I}_{e(n+1)} = \begin{bmatrix} J_n & 0 \\ 0 & J_{n+1} \end{bmatrix}, \quad \mathbf{K}_{e(n+1)} = \begin{bmatrix} k_{n+1} & -k_{n+1} \\ -k_{n+1} & k_{n+1} \end{bmatrix}, \quad \mathbf{C}_{e(n+1)} = \begin{bmatrix} c_{n+1} & -c_{n+1} \\ -c_{n+1} & c_{n+1} \end{bmatrix},$$

$$\boldsymbol{\theta}_{e(n+1)} = \begin{Bmatrix} \theta_n \\ \theta_{n+1} \end{Bmatrix}.$$

G geared—rigid tooth mesh:

$$\mathbf{I}_{e(n+1)} = \begin{bmatrix} n_G^2 J'_n & 0 \\ 0 & J_{n+1} \end{bmatrix}, \quad \mathbf{K}_{e(n+1)} = \begin{bmatrix} n_G^2 k_{n+1} & -n_G k_{n+1} \\ -n_G k_{n+1} & k_{n+1} \end{bmatrix}, \quad \mathbf{C}_{e(n+1)} = \begin{bmatrix} n_G^2 c_{n+1} & -n_G c_{n+1} \\ -n_G c_{n+1} & c_{n+1} \end{bmatrix},$$

$$\boldsymbol{\theta}_{e(n+1)} = \begin{Bmatrix} \theta_n \\ \theta_{n+1} \end{Bmatrix}.$$

G geared—elastic tooth mesh:

$$\mathbf{I}_{e(n+1)} = \begin{bmatrix} J_n & 0 \\ 0 & J_{n+1} \end{bmatrix}, \quad \mathbf{K}_{e(n+1)} = \begin{bmatrix} r_n^2 k_{n+1} & -r_n r_{n+1} k_{n+1} \\ -r_n r_{n+1} k_{n+1} & r_{n+1}^2 k_{n+1} \end{bmatrix}, \quad \boldsymbol{\theta}_{e(n+1)} = \begin{Bmatrix} \theta_n \\ \theta_{n+1} \end{Bmatrix}.$$

Branched:

$$\mathbf{I}_{e(n+1)} = \begin{bmatrix} \frac{J_n}{2} & 0 \\ 0 & J_{n+1} \end{bmatrix}, \quad \mathbf{K}_{e(n+1)} = \begin{bmatrix} k_{n+1} & -k_{n+1} \\ -k_{n+1} & k_{n+1} \end{bmatrix}, \quad \mathbf{C}_{e(n+1)} = \begin{bmatrix} c_{n+1} & -c_{n+1} \\ -c_{n+1} & c_{n+1} \end{bmatrix},$$

$$\boldsymbol{\theta}_{e(n+1)} = \begin{Bmatrix} \theta_n \\ \theta_{n+1} \end{Bmatrix},$$

$$\mathbf{I}_{e(n+2)} = \begin{bmatrix} \frac{J_n}{2} & 0 \\ 0 & J_{n+2} \end{bmatrix}, \quad \mathbf{K}_{e(n+2)} = \begin{bmatrix} k_{n+2} & -k_{n+2} \\ -k_{n+2} & k_{n+2} \end{bmatrix}, \quad \mathbf{C}_{e(n+2)} = \begin{bmatrix} c_{n+2} & -c_{n+2} \\ -c_{n+2} & c_{n+2} \end{bmatrix},$$

$$\boldsymbol{\theta}_{e(n+2)} = \begin{Bmatrix} \theta_n \\ \theta_{n+2} \end{Bmatrix}.$$

Grounded:

$$\mathbf{I}_{e(n)} = [J_n], \quad \mathbf{K}_{e(n)} = [k_n], \quad \mathbf{C}_{e(n)} = [c_n], \quad \boldsymbol{\theta}_{e(n)} = \{\theta_n\}.$$

Grounding may also be modelled by using any element with the ground as one coordinate and after applying boundary conditions to the global matrices. The coordinate representing the ground is removed from the equations of motion.

2.1. Dynamic modelling of powertrain systems with torsional finite elements

The general finite element types presented can be used for quickly obtaining the equations of motion for large complicated systems. It can be used for any lumped inertia torsional system and is particularly useful for vehicle powertrain applications.

A simple model for a vehicle powertrain system with a *manual transmission* is the three-degree-of-freedom model of Fig. 2. The gear ratio, n , can be set for the particular gear and the model used for free vibration analysis. If the grounding on coordinate 3 is removed (stiffness and damping element 4) and a torque vector included in the equation of motion then the model can be used for forced vibration analysis. The model can be extended to include more degrees of freedom and branching to drive wheels if needed, such as for four-wheel drive versions with a differential between the differentials configuration. This model is appropriate for determining the frequency for shuffle mode.

Modelling vehicle powertrain systems fitted *automatic transmissions* can be complicated but the finite element method simplifies the task considerably. One such complexity for which the method is particularly appropriate is for powertrain systems with single stage or multi-stage planetary gear sets. Fig. 3 provides a schematic for such a system. In this system k_1, k_7, k_9 (input shaft and tire stiffness) are direct elements and k_6, k_8 are rigid geared and branched elements (drive shafts and differential gearing). The remaining connections—those in and out of the planetary gear set

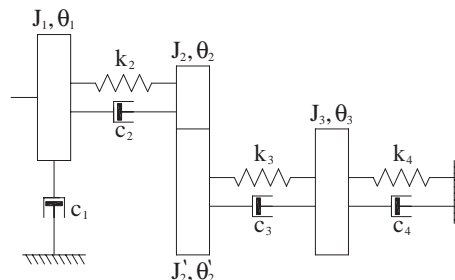


Fig. 2. Dynamic model for powertrain with manual transmission.

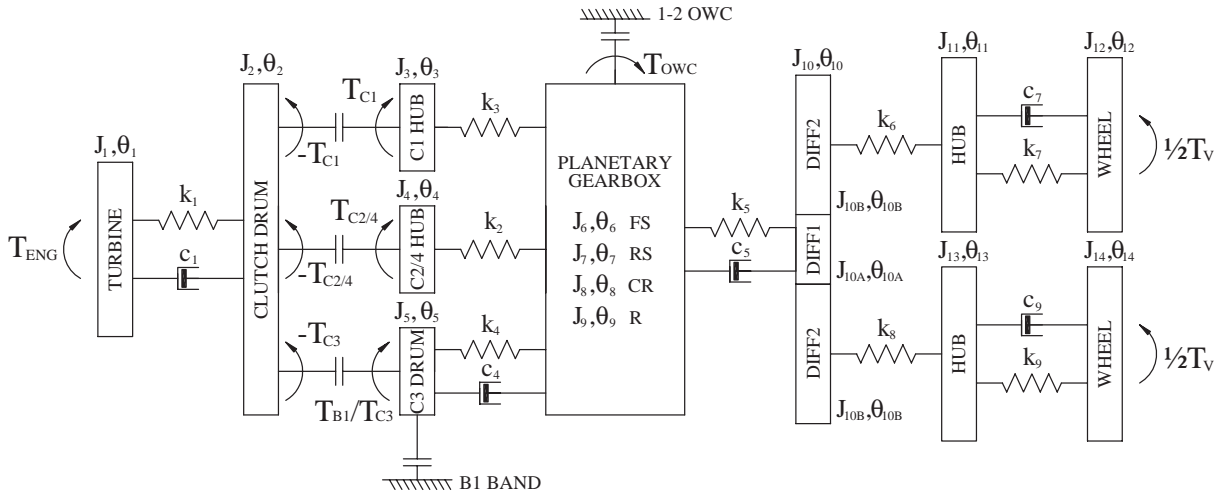


Fig. 3. Dynamic model for powertrain system with automatic transmission—all gear states.

are described by a custom finite element. The complete derivation for this element is provided by Zhang et al. [21]. Briefly, the element is derived from equations of motion for gear components that include the internal forces and external torques and from the constraining acceleration relationships between the components. The element is general and can be modified for each gear state when placed in the surrounding powertrain system. The transmission has many states of operation—first through to fourth gears and torque converter lock-up, with clutches and bands controlling gear shifts and their states defining the motion of the gear set components. Using the torsional finite elements the global system can be quickly assembled for any of these states. The final set of equations includes the complete dynamics of the planetary gear set. This same methodology can be applied to five and six speed automatic transmissions.

Continuously variable transmissions (CVTs) are the most recent type of transmission to be widely used in vehicle powertrains. Common types are toroidal, v-belt and hydromechanical CVTs. These systems can be even more complicated than automatic transmissions as some have multi-staging and some are used in tandem with planetary gear sets—then requiring clutches and/or brake bands. *The finite element method again provides an appropriate tool for the dynamic modelling of these parametric systems.* Fig. 4 presents a model for a powertrain fitted with a half toroidal CVT and planetary gear set. There are two clutches, a high-velocity clutch (HVC) which connects the toroid direct to the final drive and a low-velocity clutch (LVC) which connects the toroid to the final drive via a single stage planetary gear set. In this system the power can flow either way depending on the clutch engagement. The connection between the LVC and the ring gear (via the sun gear), k_6 and c_6 , are modelled as geared elements. Note the gear set is modelled with equivalent ring gear coordinates. The connections from the final drive to the wheels, k_9 and c_9 , and k_{10} and c_{10} , are modelled as geared and branched elements.

Torque is transferred between the toroids and the roller via a thin film of oil that transiently acts like a solid. This film can be represented with a damping and stiffness. Custom finite elements have been derived to represent this connection. Connections k_2 , c_2 and k_3 , c_3 are considered as

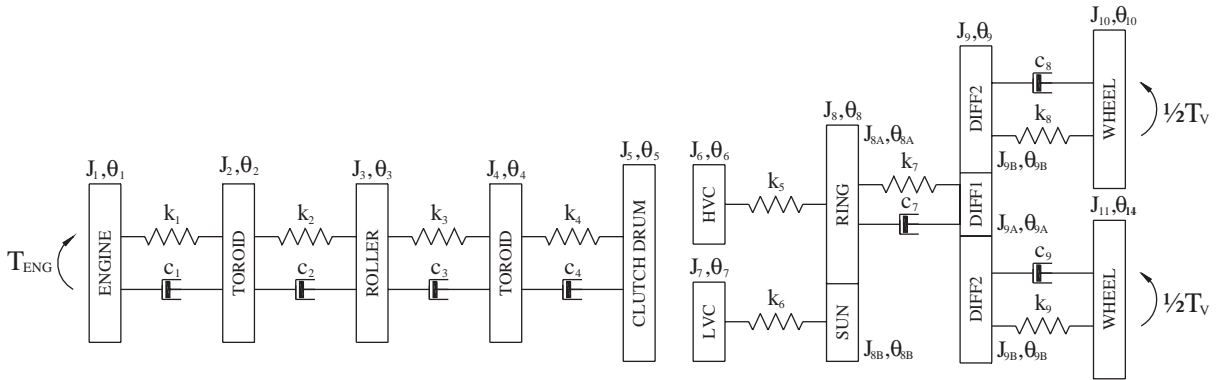


Fig. 4. Dynamic model for powertrain fitted with CVT and planetary gear set.

horizontal. With radii r_2 , r_3 and r_4 , torsional stiffness is introduced as (likewise for torsional damping):

$$k'_2 = r_3^2 k_2 \quad \text{and} \quad k'_3 = r_4^2 k_3.$$

The derived elements are:

$$\mathbf{I}_2 = \begin{bmatrix} J_2 & 0 \\ 0 & \frac{J_3}{2} \end{bmatrix}, \quad \mathbf{K}_2 = \begin{bmatrix} n_2^2 k'_2 & -n_2 k'_2 \\ -n_2 k'_2 & k'_2 \end{bmatrix}, \quad \mathbf{C}_2 = \begin{bmatrix} n_2^2 c'_2 & -n_2 c'_2 \\ -n_2 c'_2 & c'_2 \end{bmatrix}, \quad \boldsymbol{\theta}_2 = \begin{Bmatrix} \theta_2 \\ \theta_3 \end{Bmatrix}, \quad n_2 = \frac{r_2}{r_3},$$

$$\mathbf{I}_3 = \begin{bmatrix} \frac{J_3}{2} & 0 \\ 0 & J_4 \end{bmatrix}, \quad \mathbf{K}_3 = \begin{bmatrix} n_3^2 k'_3 & -n_3 k'_3 \\ -n_3 k'_3 & k'_3 \end{bmatrix}, \quad \mathbf{C}_3 = \begin{bmatrix} n_3^2 c'_3 & -n_3 c'_3 \\ -n_3 c'_3 & c'_3 \end{bmatrix}, \quad \boldsymbol{\theta}_3 = \begin{Bmatrix} \theta_3 \\ \theta_4 \end{Bmatrix}, \quad n_3 = \frac{r_3}{r_4}.$$

Note coordinate 2 and 4 have positive rotation clockwise. Coordinate 3 has positive rotation anti-clockwise.

All other connections in the system are direct elements. The global system can be quickly assembled from these elements with a global coordinate vector for either low- or high-velocity clutch engagement. Simulations can be programmed for transient dynamics by using time varying radii. For powertrains fitted with toroids and planetary gears the transient dynamics for clutch engagement together with CVT ratio change can be modelled by use of these elements and a finite element for the planetary gear set [21]. This can be achieved by using a rigid geared element for the planetary motion and importing the gear ratio change for both the CVT and planetary elements.

3. Dynamic model with clutch engagement and gear lash nonlinear dynamics

Fig. 5 presents a dynamic model for investigating clutch engagement and gear lash nonlinear dynamics. Six degrees of freedom are modelled—engine, clutch drum, clutch hub, final drive ring

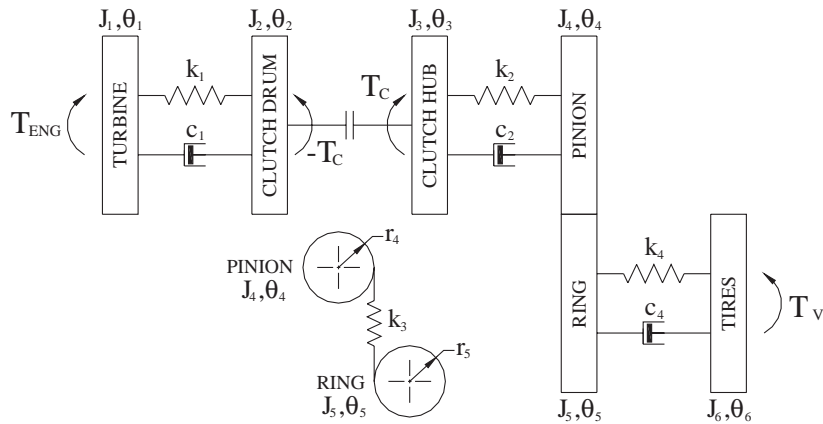


Fig. 5. Dynamic model for powertrain with clutch engagement and gear lash nonlinearities.

Table 1
System parameters

Parameter	Value	Parameter	Value
J_1	0.25 kg m ²	k_3/k_m	1e8 N m
J_2	0.001 kg m ²	k_4	10 000 N m/rad
J_3	0.001 kg m ²	c_1	2 N m s/rad
J_4	0.005 kg m ²	c_2	0.5 N m s/rad
J_5	0.015 kg m ²	c_4	4 N m s/rad
J_6	70 kg m ²	r_4	0.0218 m
k_1	10 000 N m/rad	r_5	0.0675 m
k_2	30 000 N m/rad	r_5	0.0005 m

and pinion gear, and tire/vehicle mass. The four stiffness elements are input shaft, propeller shaft, tooth mesh and drive shaft. The system parameters given in Table 1 are approximate to a passenger car. Transmission gearing is assumed as 1:1 and ignored, transmission inertia is lumped to the clutch hub. This model is simplified to more clearly illustrate simulation techniques and the causes and effects of these nonlinearities in powertrain systems. The technique can be applied in particular vehicle configurations—see Section 6.

The finite element inertia, stiffness and damping matrices and local coordinate vectors for this system are:

$$\mathbf{I}_{e1} = \begin{bmatrix} J_1 & 0 \\ 0 & J_2 \end{bmatrix}, \quad \mathbf{K}_{e1} = \begin{bmatrix} k_1 & -k_1 \\ -k_1 & k_1 \end{bmatrix}, \quad \mathbf{C}_{e1} = \begin{bmatrix} c_1 & -c_1 \\ -c_1 & c_1 \end{bmatrix}, \quad \theta_{e1} = \begin{cases} \theta_1 \\ \theta_2 \end{cases}, \quad \theta_{e1} = \begin{cases} \theta_1 \\ \theta_{2,3} \end{cases}, \quad (1a)$$

$$\mathbf{I}_{e2} = \begin{bmatrix} J_3 & 0 \\ 0 & 0 \end{bmatrix}, \quad \mathbf{K}_{e2} = \begin{bmatrix} k_2 & -k_2 \\ -k_2 & k_2 \end{bmatrix}, \quad \mathbf{C}_{e2} = \begin{bmatrix} c_2 & -c_2 \\ -c_2 & c_2 \end{bmatrix}, \quad \boldsymbol{\theta}_{e2} = \begin{Bmatrix} \theta_3 \\ \theta_4 \end{Bmatrix}, \quad \boldsymbol{\theta}_{e2} = \begin{Bmatrix} \theta_{2,3} \\ \theta_4 \end{Bmatrix}, \quad (1b)$$

$$\mathbf{I}_{e3} = \begin{bmatrix} J_4 & 0 \\ 0 & J_5 \end{bmatrix}, \quad \mathbf{K}_{e3} = \begin{bmatrix} r_4^2 k_3 & -r_4 r_5 k_3 \\ -r_4 r_5 k_3 & r_5^2 k_3 \end{bmatrix}, \quad \boldsymbol{\theta}_{e3} = \begin{Bmatrix} \theta_4 \\ \theta_5 \end{Bmatrix}, \quad \boldsymbol{\theta}_{e3} = \begin{Bmatrix} \theta_4 \\ \theta_5 \end{Bmatrix}, \quad (1c)$$

$$\mathbf{I}_{e4} = \begin{bmatrix} 0 & 0 \\ 0 & J_6 \end{bmatrix}, \quad \mathbf{K}_{e4} = \begin{bmatrix} k_4 & -k_4 \\ -k_4 & k_4 \end{bmatrix}, \quad \mathbf{C}_{e4} = \begin{bmatrix} c_4 & -c_4 \\ -c_4 & c_4 \end{bmatrix}, \quad \boldsymbol{\theta}_{e4} = \begin{Bmatrix} \theta_5 \\ \theta_6 \end{Bmatrix}, \quad \boldsymbol{\theta}_{e4} = \begin{Bmatrix} \theta_5 \\ \theta_6 \end{Bmatrix}. \quad (1d)$$

The finite element matrices are assembled into global system matrices by using local coordinate vectors and the global coordinate vector. When the clutch is disengaged or slipping the system has six degrees of freedom. When the clutch is engaged the system has five degrees of freedom, either coordinate 2 or 3 can represent the engaged clutch inertia. The final equation of motion for the system will have the form:

$$\mathbf{I}\ddot{\boldsymbol{\theta}} + \mathbf{C}\dot{\boldsymbol{\theta}} + \mathbf{K}\boldsymbol{\theta} = \mathbf{T}. \quad (2)$$

With global coordinate vectors:

$$\boldsymbol{\theta} = \{\theta_1 \quad \theta_2 \quad \theta_3 \quad \theta_4 \quad \theta_5 \quad \theta_6\} \quad \text{clutch slipping}, \quad (3)$$

$$\boldsymbol{\theta} = \{\theta_1 \quad \theta_{2,3} \quad \theta_4 \quad \theta_5 \quad \theta_6\} \quad \text{clutch engaged}. \quad (4)$$

And torque vectors:

$$\mathbf{T} = \{T_E \quad T_C \quad -T_C \quad 0 \quad 0 \quad -T_V\} \quad \text{clutch slipping}, \quad (5)$$

$$\mathbf{T} = \{T_E \quad 0 \quad 0 \quad 0 \quad -T_V\} \quad \text{clutch engaged}. \quad (6)$$

3.1. Linear analysis

For free vibration analysis, the tire/vehicle inertia coordinate can be grounded or free-spinning, it makes little difference as the effective vehicle inertia is so large compared to the rest of the system. The system can be linearised by setting the torque vector to zero and omitting gear lash. If it is free spinning the eigenvalues of the system have a zero value or pair, representing the rigid body motion of the system, the mode shape reflects the gear ratio. The five-degree-of-freedom system (engaged clutch) is fully coupled whereas the six-degree-of-freedom system is uncoupled at the disengaged/slipping clutch. For either configuration there are four natural frequencies and corresponding mode shapes.

Clutch engagement judder has been investigated for the powertrain with automatic transmission configuration of Fig. 3 [15]. The clutch torque is represented as a function of clutch geometry, applied pressure and the sliding friction coefficient. The system can be linearised for the

slipping clutch by assuming a constant applied pressure and defining the friction coefficient as a linear function of clutch relative velocity. The clutch torque is then autonomous as it is described by a constant and a function of relative velocity. The magnitude and sign of the relative velocity function is dependent on the gradient of the friction coefficient. The variation of the friction coefficient is equivalent to viscous damping. If the gradient is positive/negative the roots of the system are stable/unstable. Other damping elements can stabilise the system.

3.2. Nonlinear analysis

Nonlinear analysis includes:

- Engine torque as a function of engine speed and throttle position.
- Clutch torque as a function of apply pressure and the sliding friction coefficient.
- Clutch engagement stick/slip piecewise analysis.
- Gear mesh clearance nonlinearity.

The engine torque can be described by an engine characteristic map for a typical four cylinder gasoline engine. The engine torque is a function of the engine speed and the throttle position.

Assuming constant pressure across the surface of the clutch plates, the equation for clutch torque is:

$$T_C = N_s R_m \mu_S F, \quad (7)$$

where N_s is the number of friction surfaces, R_m is the clutch mean radius, μ_S the coefficient of sliding friction and F the clutch actuating force. The actuating force is determined from applied pressure which is nonlinear and a function of time. The mean clutch radius is determined from the clutch outside (r_o) and inside (r_i) radii:

$$R_m = \frac{2(r_o^3 - r_i^3)}{3(r_o^2 - r_i^2)}. \quad (8)$$

3.2.1. Clutch stick–slip—friction nonlinearity

When the clutch engages the system changes state as there is one less degree of freedom. If there is not enough holding torque the clutch may slip again. An algorithm has been used to model this clutch stick–slip. In numerical simulations the algorithm determines the state of the system at every time step. The numerical solution is piecewise and nonlinear. The state is determined by first checking the slip speed inequality and then if necessary checking the holding torque versus shearing torque inequality. The equations of motion for each state, sliding or engaged clutch (stichon) are then solved as dictated. Whilst sliding the direction of sliding dictates the sign of the clutch torque. If the system commences sliding from stichon, the sign of the clutch torque needs to be determined from the torque flow in the system.

T_C is a nonlinear friction torque, a function of sliding velocity and the normal force:

$$T_C = \begin{cases} \operatorname{sgn}(\dot{\theta}_2 - \dot{\theta}_3)T_S & \text{if } |(\dot{\theta}_2 - \dot{\theta}_3)| \geq \varepsilon_{\text{tol}}, \\ \operatorname{sgn}(T_{\text{INT}})T_S & \text{if } |(\dot{\theta}_2 - \dot{\theta}_3)| < \varepsilon_{\text{tol}} \text{ and } T_{ST} < |T_{\text{INT}}|, \\ T_{\text{INT}} & \text{if } |(\dot{\theta}_2 - \dot{\theta}_3)| < \varepsilon_{\text{tol}} \text{ and } T_{ST} \geq |T_{\text{INT}}|, \end{cases} \quad (9)$$

where ε_{TOL} is the tolerance of zero velocity for numerical simulations and T_S and T_{ST} are clutch slipping and holding torques (dependent on kinetic and static friction, respectively).

The clutch slipping torque is:

$$T_S = N_s R_m \mu_S F. \quad (10)$$

The clutch-holding torque, T_{ST} , is the same equation with the sliding coefficient of friction replaced with the static coefficient, μ_{S0} .

In stichon, the shearing torque, T_{INT} , between clutch plates is difficult to calculate exactly. When each side is modelled separately the *slipping* equations (global coordinate vector (3)) apply with the clutch torque in the torque vector (5) set as the *unknown* shearing torque. We now have two unknowns in individual equations for coordinates 2 and 3, *angular acceleration* and *clutch torque*—they cannot be solved for T_C . When combining the two equations the shearing torque is cancelled—providing the engaged clutch system with global coordinate vector (4). However, the shearing torque can be found numerically for a reasonably accurate solution. This is achieved by using the acceleration value from the proceeding time step as an approximation so as to solve the equations for an approximate value of T_C , in this case actually T_{INT} . Using this method a fine time step is required around the point of interest.

Thus the shearing torque can be determined via the equation for coordinate 2,

$$T_{\text{INT}(t)} = -J_2 \ddot{\theta}_{2(t-1)} + k_1(\theta_{1(t)} - \theta_{2(t)}) + c_1(\dot{\theta}_{1(t)} - \dot{\theta}_{2(t)}) \quad (11)$$

or via the equation for coordinate 3,

$$T_{\text{INT}(t)} = J_3 \ddot{\theta}_{3(t-1)} + k_2(\theta_{3(t)} - \theta_{4(t)}) + c_2(\dot{\theta}_{3(t)} - \dot{\theta}_{4(t)}). \quad (12)$$

Eqs. (11) and (12) can be combined to:

$$T_{\text{INT}(t)} = \frac{1}{2} [J_3 \ddot{\theta}_{3(t-1)} - J_2 \ddot{\theta}_{2(t-1)} + k_1(\theta_{1(t)} - \theta_{2(t)}) + c_1(\dot{\theta}_{1(t)} - \dot{\theta}_{2(t)}) + k_2(\theta_{3(t)} - \theta_{4(t)}) + c_2(\dot{\theta}_{3(t)} - \dot{\theta}_{4(t)})]. \quad (13)$$

In simulations the flow of Eqs. (11)–(13) can be compared to assess error. This is critical in the region where the value of T_{INT} , determines the state of the system. Reducing the time step so the difference between values is minimal is essential. When slipping the value of T_{INT} can also be calculated in the same way it should practically equal the applied clutch torque.

3.2.2. Gear lash—contact nonlinearity

Gear lash is the clearance between mating gears that is required for their smooth rotation. In a loaded system meshing gears can lose contact during torque reversal. Within a certain range of lash the system is disconnected and the gear mesh stiffness is zero. When the gears reengage the mesh stiffness is a combination of tooth bending and material compression, the impact causes

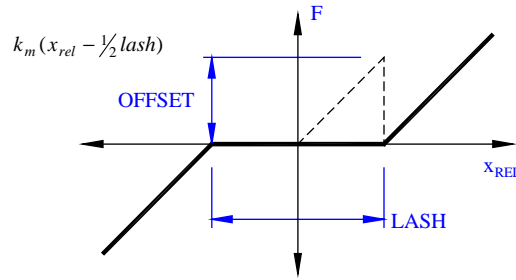


Fig. 6. Nonlinear gear mesh function.

transient vibration and noise. The nonlinear stiffness can be presented as restoring force as a function of relative position as shown in Fig. 6. The algorithm used to model the gear lash is:

For mesh stiffness:

$$k_3 = \begin{cases} k_m & \text{if } |(x_{rel})| \geq \frac{lash}{2}, \\ 0 & \text{if } |(x_{rel})| < \frac{lash}{2}, \end{cases} \quad (13)$$

where

$$x_{rel} = r_4\theta_4 - r_5\theta_5. \quad (14)$$

With the spring force, F , nonlinear in this way the torque vector is needed to account for the offset of force from the zero position. The global torque vectors (5) and (6) are modified to include the torque offset:

$$T = \{ T_E \quad T_C \quad -T_C \quad T_4 \quad T_5 \quad -T_V \} \quad \text{clutch slipping}, \quad (15)$$

$$T = \{ T_E \quad 0 \quad T_4 \quad T_5 \quad -T_V \} \quad \text{clutch engaged}, \quad (16)$$

where

$$T_4 = -\text{sign}(x_{rel})r_4k_3 \frac{lash}{2} \quad \text{and} \quad (17)$$

$$T_5 = \text{sign}(x_{rel})r_5k_3 \frac{lash}{2}. \quad (18)$$

When the stiffness, k_3 , is found to be zero, the torque offset is returned as zero.

4. Numerical simulation

Numerical simulations have been programmed in Matlab for the powertrain system of Fig. 3. The simulation is for clutch engagement and includes the stick–slip and gear lash algorithms. This simulation of engaging clutch is similar to the inertia phase from planetary gear dynamics in automatic transmission gear shifting. The simulations are not intended to closely model a

particular powertrain system rather to demonstrate the effectiveness and the robustness of the algorithms and dynamic models. The methodology can be applied to specific powertrain systems such as presented in Figs. 4 and 5 to closely model a particular vehicles powertrain dynamics. These models of Figs. 4 and 5 can naturally be extended with more detail such as tire slip, combustion processes, etc.

The numerical simulation is transient and piecewise. The solution to the equations of motion (2) is solved across engaged and disengaged states, with the system of equations and torque vector changing as the gear state changes. The systems external torques or forcing functions are the inputs into the model and define the shifting process. The equations of motion are reduced to first order for use with the solver. The stick–slip algorithm (9) is applied to determining if there is any stick–slip on clutch engagement—the transition from sticking to slipping is piecewise (engaged/disengaged clutch). The gear lash algorithm is applied to determine if there is any backlash from restoring torque transients. The solver used was Matlab’s ODE15s which is appropriate for stiff systems. Modifications were made to the solver to allow more control of time stepping and for programming algorithms as necessary. Matlab provides a concise summary of the solver:

‘ODE15S is a quasi-constant step size implementation in terms of backward differences of the Klopfenstein–Shampine family of Numerical Differentiation Formulas of orders 1–5. The natural “free” interpolants are used. Local extrapolation is not done. By default, Jacobians are generated numerically.’

For numerical modelling with the CVT powertrain (Fig. 4) the torsional elements include speed ratio parameters or radii. If the ratio is varied the system matrices become time variant. This type of parametric system is highly nonlinear and can be difficult with solvers. Control of the time stepping is important.

Assumptions made for the simulations are as follows:

- Engine torque is interpolated from the engine torque map at 40% throttle with added harmonics for a typical four cylinder engine (Fig. 7). At 40% throttle the engine torque is fairly constant for the engine speeds in this simulation.
- Clutch pressure is already applied yielding 200 N m torque and increases linearly with time with added oscillations at 45 Hz (Fig. 7). The oscillations are not modelled from a real hydraulic

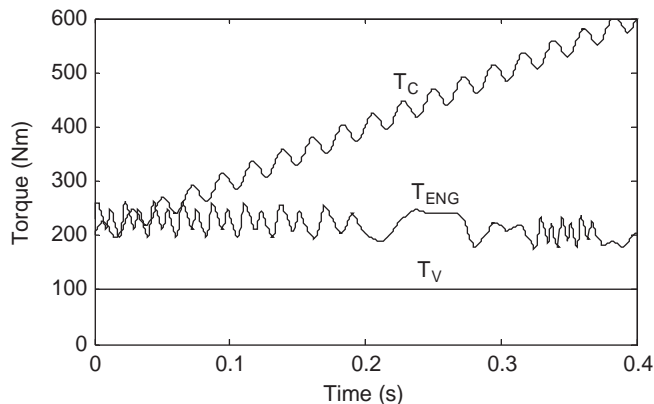


Fig. 7. Engine, clutch and vehicle torques.

system or determined from clutch judder but are used to easily induce the system response needed to demonstrate the stick–slip phenomena. Both the hydraulic system and the friction characteristics can induce torque oscillations in real systems.

- Vehicle aerodynamic drag, rolling resistance and gradient torques are combined and set to a constant value of 100 N m (Fig. 7).
- Viscous damping is minimal to provide larger transients to easier illustrate the stick–slip and gear lash.
- A small value (0.01 N m) is added to the clutch pressure torque due to numerical issues (see Section 6).
- Gear lash is set at 0.5 mm.
- The tolerance of relative velocity for the stick–slip algorithm is set at ± 0.01 rad/s (see Section 6).

The initial conditions for the simulation are determined to provide balanced spring torque. There is no stiffness connection between each side of the engaging clutch thus the clutch drum and hub are set zero absolute displacement and the other coordinates angular displacements are calculated relative to these coordinates. They are denoted the ‘upstream’ (engine side) and ‘downstream’ (tire side) sides of the clutch. The initial condition angular velocities are predetermined for upstream and downstream sides for zero relative velocity across damping elements. The rigid body acceleration of the system needs to be accounted for and is calculated as follows:

Upstream:

$$\ddot{\theta}_{1,2} = \frac{(T_{\text{ENG}} - T_C)}{J_1 + J_2}. \quad (19)$$

Downstream:

$$\ddot{\theta}_{3,4} = \frac{(T_C - r_4/r_5 T_V)}{J_3 + J_4 + (r_4/r_5)^2 (J_5 + J_6)}, \quad (20)$$

$$\ddot{\theta}_{5,6} = \ddot{\theta}_4 \left(\frac{r_4}{r_5} \right). \quad (21)$$

The angular displacements of the remaining coordinates are calculated as follows:

Upstream:

$$\theta_2 = 0, \quad (22)$$

$$\theta_1 = -\frac{(J_1 \ddot{\theta}_1 - T_{\text{ENG}})}{k_1}. \quad (23)$$

Downstream:

$$\theta_3 = 0, \quad (24)$$

$$\theta_4 = \frac{(J_3 \ddot{\theta}_3 - T_C)}{k_2}, \quad (25)$$

$$\theta_5 = \frac{(J_4\ddot{\theta}_4 + k_2\theta_4 + r_4^2k_3\theta_4)}{r_4r_5k_3}, \quad (26)$$

$$\theta_6 = \frac{(J_5\ddot{\theta}_5 - r_1r_2k_3\theta_4 + r_4^2k_3\theta_5 + k_4\theta_5)}{k_4}. \quad (27)$$

Eq. (27) can be verified with:

$$\theta_6 = -\frac{(J_6\ddot{\theta}_6 - k_4\theta_5 + T_V)}{k_4}. \quad (28)$$

The viscous damping can be omitted in calculating the initial condition as the relative velocity over viscous damping elements is zero. The angular displacements are calculated with the gear mesh stiffness linearised, i.e. no lash. The lash must then be subtracted from the coordinates downstream of the gear mesh in terms of angular displacement:

$$\theta_5 \text{ (adjusted)} = \theta_5 - \frac{\text{lash}/2}{r_5}, \quad (29)$$

$$\theta_6 \text{ (adjusted)} = \theta_6 - \frac{\text{lash}/2}{r_5}. \quad (30)$$

This method must be used to calculate the initial conditions as the system of equations of motion have no stiffness connection between the clutch facings. Determining the initial conditions via matrix calculations is not possible as the stiffness matrix is singular. Finding balanced initial conditions become even more complex with planetary gears such as the system of Fig. 3.

The initial conditions for the simulations are given in Table 2.

When using the stick–slip algorithm the tolerance of zero relative velocity needs to be carefully adjusted along with the time step for error free simulations. If the solution points for the clutch relative velocity pass the zero crossing without falling within the tolerance the solution will be erroneous. For these simulations the tolerance, ε_{TOL} , was set at ± 0.01 rad/s. The time step was set initially with maximum step of 0.25 ms (10 points in a 400 Hz wave) and once the solution time reached 0.2 s it is reduced as a linear function of relative velocity to 0.025 ms at 0.25 s. After the first stick point the time step is held at this value until the solution is finished—as the clutch may slip again. This allows a faster simulation where finer time steps are not required and greater accuracy as the zero crossing point is approached.

Table 2
Initial conditions

Angular displacements	Value	Angular velocities	Value
Engine	0.0201	Engine	300
Clutch drum	0	Clutch drum	300
Clutch hub	0	Clutch hub	150
Diff pinion	−0.0067	Diff pinion	150
Diff ring	−0.0072	Diff ring	48.4
Tires	−0.06909	Tires	48.4

The gear lash algorithm also requires a fine time step as the gear mesh is quite stiff and impacts cause high-frequency transients. In these simulations the impacts are likely after clutch engagement and the time step is already reduced in this region for the stick–slip algorithm. Using appropriate time stepping is one of the trickier parts of this type of simulations. With the power of modern computers it is easier to just set fine time steps to begin with. However, when the degrees of freedom for these types simulations are increased, such as with more complex models (Fig. 3), computing time increases significantly and the adjustments to time stepping speed up research work. Damping is another factor which significantly reduces computation time. If high-frequency modes in large degree-of-freedom stiff systems are not damped computation times can be much longer depending on solver accuracy.

The piecewise transition between the six- and five-degree-of-freedom systems can also be tricky. The equations of motion model the rigid body motion as well as the elastic system. Each side of the clutch rotates through different absolute angular displacements when the clutch is slipping, thus when the clutch sticks an angular displacement offset must be subtracted from the upstream side of the clutch. The offset is determined to give zero relative angular displacement between sticking clutch surfaces. This must be done at the first stick time and each time the clutch slips and sticks again. With this approach in the numerical simulations the elastic dynamics of the system are correctly preserved over the piecewise transition, without the solution will take an exponential path and the solver may crash or stall. Similarly, programmers must be careful when using a tolerance of zero velocity. In this simulation the relative velocity is set to zero after stichon from whatever value fell within the tolerance, the difference is the velocity offset. The offset is added/subtracted to all coordinates upstream of the clutch so as not to add/subtract energy from the system. Also a small value (0.01 Nm) is added to the clutch-holding torque in algorithm (9). At first time step from entering the zero tolerance region small error in the estimate of the shearing from the previous timestep. The error can cause the system to exhibit slip when it should not. Increasing the holding torque this small amount is enough to offset the error and is too small to affect the solution.

To make the programming of the piecewise simulation simpler, the number of degrees of freedom is maintained at six by use of a dummy coordinate when the degrees of freedom should be five for the whole simulation. When the clutch is engaged, i.e., the five-degree-of-freedom system, the coordinates for each side of the clutch (coordinates 2 and 3) are both modelled as the engaged clutch. The coordinates have the same solution and each represent the combined inertia of the clutch drum and hub. Each coordinate has the same equation of motion. With this approach the solver can be run continuously over the whole simulation. Computing time is not significantly effected. This is not appropriate to modal analysis, however with caution it can save a lot of programming time in numerical simulations.

5. Results

Free vibration analysis and transient vibration numerical simulation results are presented. The system modelled is that of Fig. 5 with system parameters of Table 1.

5.1. Free vibration analysis

Free vibration analysis was performed for both the engaged and disengaged systems. The systems of equations used a linearised tooth mesh. The standard eigenvalue problems were solved for undamped and damped systems. The natural frequencies, natural mode shapes, damped frequencies and damping ratios are given in Tables 3 and 4. Rigid body modes were returned for both systems, for the engaged system, the rigid body motion of the all degrees of freedom including gear ratio. For the disengaged system, the rigid body motion of the upstream and downstream systems.

The model is only an approximate representation of the system, i.e. a lumped mass model with four stiffness elements. The four frequencies found are representative of frequencies found in powertrain systems. 9.3 Hz is a global mode—the shuffle mode. It is associated mainly with driveshaft stiffness and engine and tire inertia. 100, 400 and 1000 Hz (engaged system) are typical high-frequency components. Due to the simplification of the clutch engagement and transmission the three lowest frequencies are moved higher when the engine mass and input shaft are disconnected. In particular the shuffle mode moves from 9.3 to 39 Hz.

Table 3
Engaged systems natural modes

Frequency (Hz)	1031.4	393.59	106.49	9.31	0
Engine	0.00	0.00	−0.09	−1.00	1.00
Clutch	−0.04	−0.36	0.94	−0.91	1.00
Pinion	1.00	1.00	1.00	−0.88	1.00
Ring	−0.89	0.39	0.32	−0.28	0.32
Tires	0.00	0.00	0.00	0.01	0.32
Damped frequency	1017	388	104	9.20	
Damping ratio (%)	1.70	3.69	7.21	1.08	

Table 4
Disengaged systems natural modes

Frequency (Hz)	1032.3	432.83	162.31	39.338	0	0
Engine	0.00	0.00	−0.04	0.00	1.00	0.00
Clutch drum	0.00	0.00	1.00	0.00	1.00	0.00
Clutch hub	−0.08	−0.68	0.00	1.00	0.00	1.00
Pinion	1.00	1.00	0.00	0.98	0.00	1.00
Ring	−0.89	0.41	0.00	0.31	0.00	0.32
Tires	0.00	0.00	0.00	0.00	0.00	0.32
Damped frequency	1019	427	160	38.9		
Damping ratio (%)	1.70	3.16	4.80	1.70		

5.2. Numerical simulation for transient vibration

The simulation for transient vibration was performed for clutch engagement with stick–slip and gear lash as described in Sections 3 and 4. The system of equations of motion are assembled as (2) with finite elements (1) and global coordinates (3)—disengaged system or (4)—engaged system. The torque vectors (5) and (6) have been adjusted for the gear lash function to (15) and (16). The simulation is piecewise around global coordinate vectors (3) and (4) according to the stick–slip function (9). The forcing functions, engine torque, clutch engagement torque and vehicle torque are presented in Fig. 7. The plot shows the engine harmonics, (dependent on engine speed) and rising clutch torque with oscillations (modelled with rising pressure). The component speeds are presented in Fig. 8. The engine and clutch drum both slow over the clutch engagement which takes around 0.3 s. This is similar to the inertia phase of an automatic transmission gear shift with clutch engagement. This is where the justification of the already applied clutch torque can be seen—in an automatic transmission the clutch torque is typically 100–200 N m at the end of the torque phase (start of the inertia phase—where gear ratios begin to change) [21]. Engagement speeds are typically 0.3–0.5 s depending on the gear shift.

The results exhibit both stick–slip and gear rattle. As mentioned in Section 3, the piecewise analysis requires the absolute displacement of the engine and clutch drum speeds to be offset on piecewise transition. Fig. 9 illustrates the offset. While the clutch is engaging the upstream and downstream sides of the disengaged system exhibits strong vibrations at 45 Hz, forced by clutch pressure oscillations. These oscillations can be seen clearly in the relative displacement plots for shaft elements (Figs. 10–12). The oscillations and the change in state at clutch engagement cause transients at 9 and 110 Hz, these correspond to the natural modes of the system when engaged. The large transients contribute to stick–slip at the clutch interface. When the relative velocity of the clutch first reaches zero (within the tolerance of zero) the clutch sticks. Due to the transients the clutch shearing torque exceeds the clutch-holding torque and the clutch breaks away. Stick time was approximately 3 ms (Fig. 13). After 0.015 s of slipping the clutch engages again. This time the transient oscillations have decayed enough for the shearing torque remaining lower than the holding torque and thus the clutch remains engaged. The occurrence of stick–slip is dependent

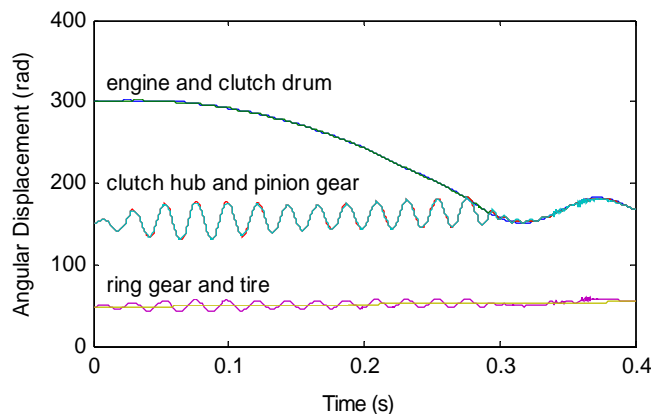


Fig. 8. Angular velocities of powertrain components.

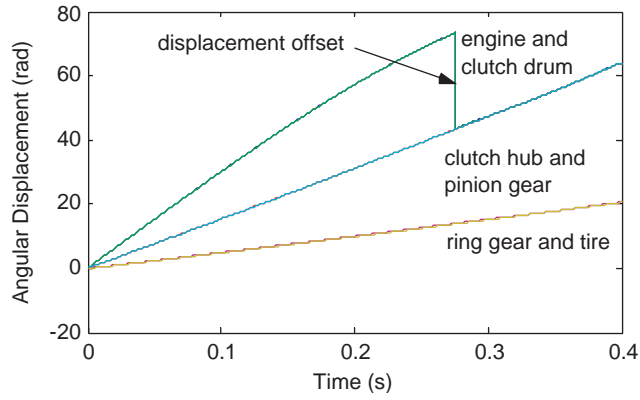


Fig. 9. Engine, clutch and vehicle torques.

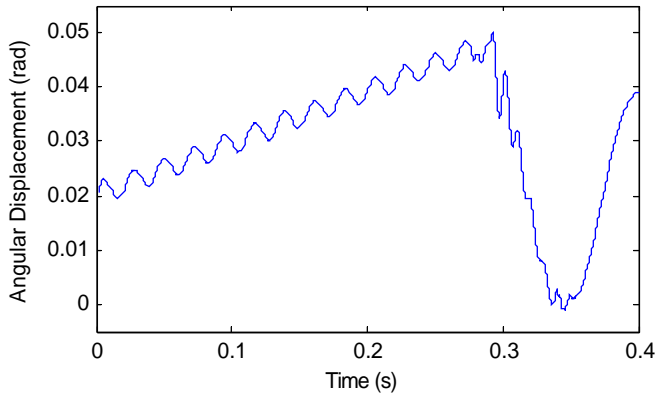


Fig. 10. Relative ang. disp.—engine and clutch hub.

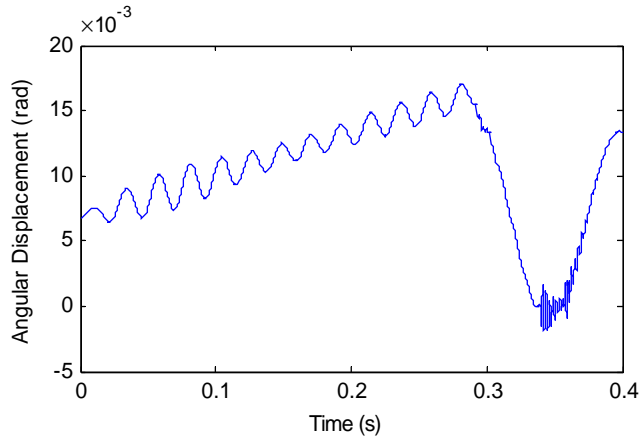


Fig. 11. Relative ang. disp.—clutch drum and pinion gear.

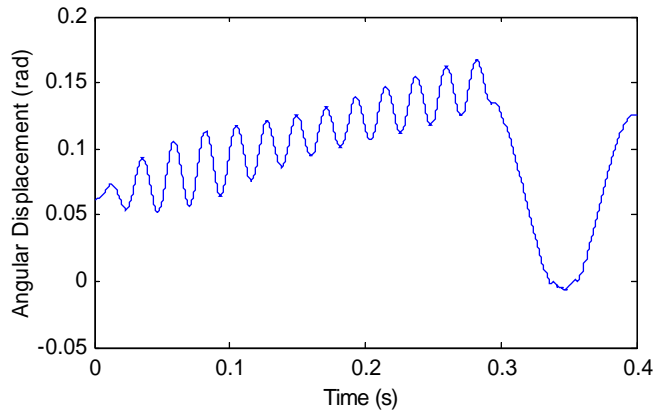


Fig. 12. Relative ang. disp.—ring gear and tire.

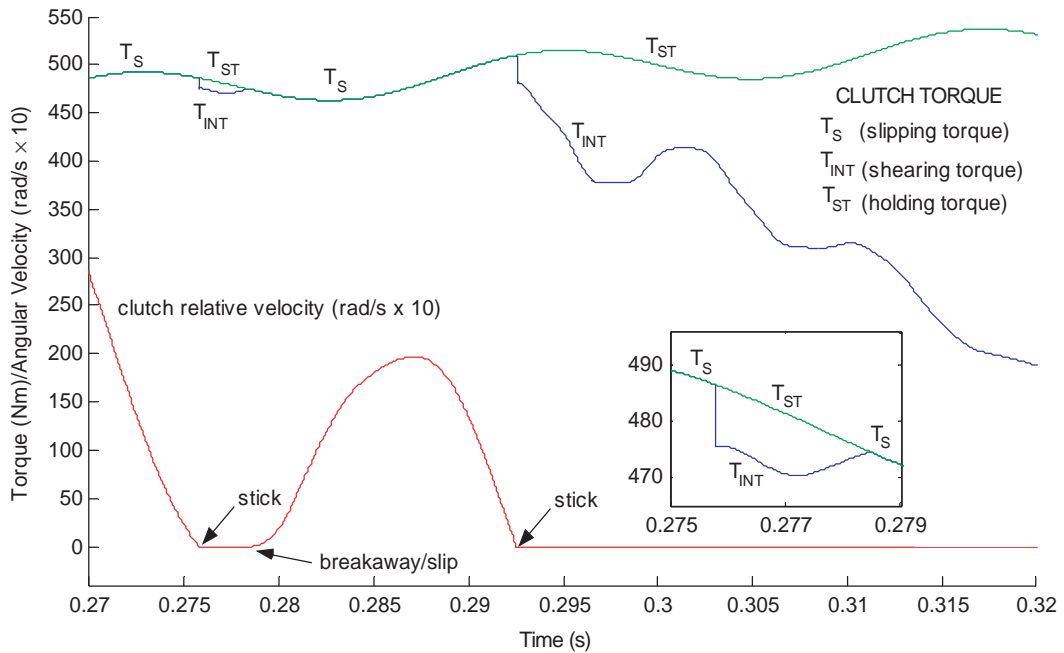


Fig. 13. Clutch slipping, shearing and holding torques versus clutch relative velocity.

on the system dynamics and engine torque and clutch apply pressure or torque. The coefficient of friction and clutch judder have a large part to play. In Ref. [15] there is further analysis of the effects of these parameters.

The shuffle mode transient from clutch engagement is large enough to cause a torque reversal in the restoring torque of the elastically modelled gear tooth mesh. During the torque reversal the gear teeth separate through the range of lash. Fig. 14 illustrates the phenomena. When the gear teeth impact on either side of the clearance high-frequency transients occur (clonk). The *backlash*

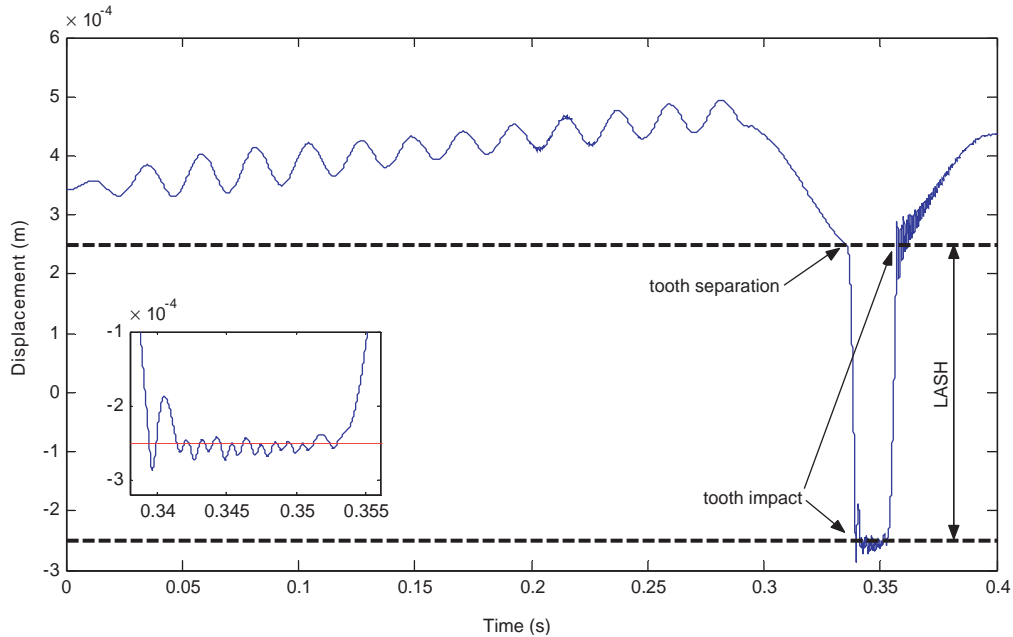


Fig. 14. Tooth mesh relative position and magnified inset around first tooth impact.

causes high-frequency transients from the 1000 Hz natural mode to be excited. The high-frequency impacts with decay of around 10 ms for the first clonk and 20 ms for the final clonk. These are similar to that found in discussed experiments for a load reversal test [20] and shock load test [17]. Clonk durations have been also noted as 25–50 ms [6,18]. For the same simulation with the damping of the high-frequency mode reduced to from 1.70% to 1.45% the decay was around 30 ms for the second clonk. A phase plane diagram (Fig. 15) has been used to illustrate the flow of the solution for this nonlinearity. The diagram shows the relative displacement versus the relative velocity for the tooth mesh. Both parameters are based on two degrees of freedom, coordinates 4 and 5 (pinion and ring), and using relative motion the dimensions are reduced from four to two. The flow of the solution starts from the right side and travels in nonlinear loops from forced vibration until the clutch engagement transient causes the torque reversal. The solution is distinctly different during the region of zero stiffness compared to that of tooth stiffness. Within zero stiffness the change in displacement precipitates less change in velocity after clear separations. After tooth impacts the solution decays in a stable nonlinear spiral like formation across the mesh transition. The transient torque from the lower frequency modes of oscillation interact with the nonlinear dynamics of the tooth mesh taking the solution in a nonlinear fashion from one forced set of spirals/loops to another. When the transient oscillations decay enough for the gears stop rattling and while the system is still driven by the engine the solution moves back to a right-hand side loops. If all vibration decays the solution will be dictated only by the rigid body torque flow of the system. This illustrates the effect of the gear lash on the dynamic solution and how low-frequency transient vibration affects occurs of lash. The system is nonlinear and the phase plane diagram does not show any limits of the solution. The

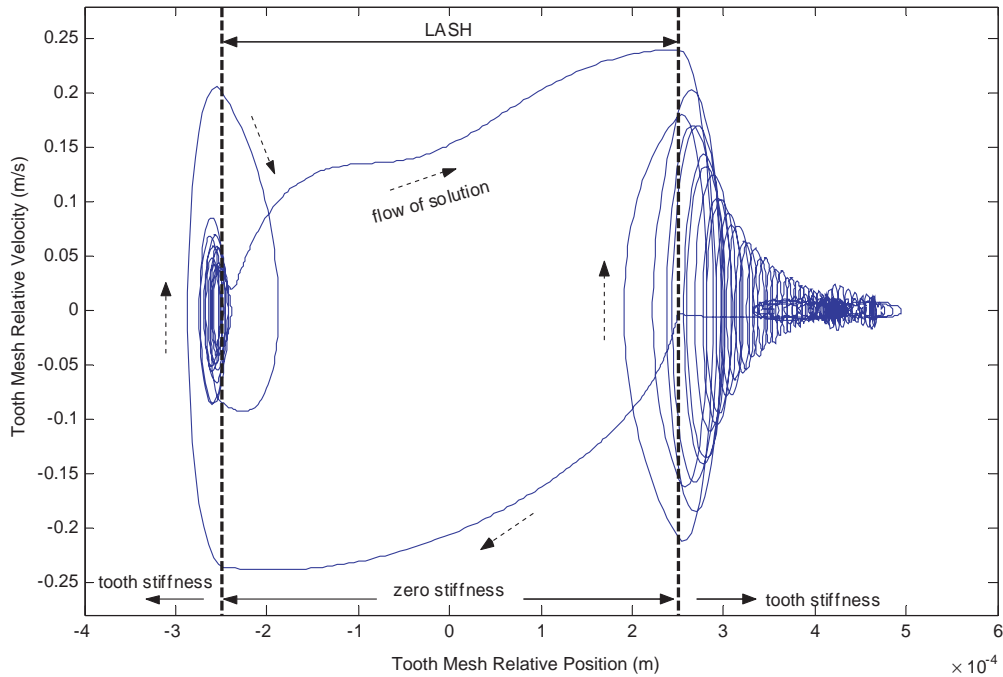


Fig. 15. Phase plane diagram—tooth mesh relative position versus relative velocity.

solution is dictated by the forcing function, nonlinear algorithms, natural modes and initial conditions.

6. Discussion

The principle aim of this report was to illustrate a numerical approach to modelling the nonlinear phenomena that is part of vehicle powertrain dynamics. How the finite element method can be used to model various powertrains to detailed levels (Figs. 3 and 4) is illustrated. Custom elements can be developed for planetary gear dynamics rigid gears [21] and in the same fashion for final drive dynamics. Gear lash elements can be introduced to these dynamics; for both a two stage planetary gear set and conventional final drive 6×6 custom finite elements are used with elastic nonlinear tooth mesh (to be reported), transient numerical simulations use the same approach for stick–slip and rattle. For gear shifting, apply torque equations with experimentally determined friction coefficients improve judder and stick–slip modelling [15]. The method can be used for manual, automatic transmission and CVT powertrains. At this point the models capture transient dynamics for shuffle, stick–slip and gear rattle as well as natural modes. They can be used for steady state, tip-in and shifting simulations. Extending the dynamic modelling is necessary for closer representation of the real system when investigating high-frequency modes and couplings between vehicle subsystems. Torque converters, tires, universal joints, etc. bring

extra complexity—forcing functions and damping are critical in most investigations of the solution to (2). For example torsional lumped mass models for tires are very simplified representations and are widely used [2,3,5]. With the finite element method and presented approach powertrain models and simulations could be extended with:

- Calculated engine combustion torque from measured/modelled combustion pressure.
- Multi-degree-of-freedom engine model.
- Torque converter dynamic model using empirically determined parameters.
- Propeller shaft distributed mass element [8].
- Planetary gear dynamics with lash.
- Final drive dynamics with lash.
- Hydraulic system model.
- Tire slip and tire vehicle coupling.
- Vehicle pitch, yaw and roll dynamics.
- Universal joint rotation.

7. Conclusion

The finite element method is a useful tool for torsional vibration analysis, particularly for powertrain systems. Once an understanding of the dynamic system is gained and a lumped mass model devised then the general finite elements, direct, geared, branched and grounded, can be assigned. In some situations custom elements can be developed to handle added system complexities, such as for single or multi-stage planetary gear sets and toroid-roller contact. Using a global coordinate vector, the finite elements for inertia, stiffness and damping and their corresponding local coordinate vectors can be assembled into the equations of motion for the global system. For systems that change state often, such as transmissions with clutch shifting, global assemblies can be quickly made that govern each state.

Once the global system has been assembled the equations of motion can be used for the various investigations. *Free vibration analysis*, with the torque vector set to zero, and the wheels either grounded or linked to the vehicle mass. Gear ratios are fixed or in the case of the system with the gear set element the clutch connections and held gear set components fix the gear ratio. *Forced vibration analysis*, analytical or numerical; analytical for fixed gear states and input torques that can be handled analytically, such as harmonic or stepped, numerical for the parametric condition of gear ratio change, for input torques from mapped data—such as engine torque and other nonlinearities such as stick–slip, clutch judder and gear backlash.

Acknowledgements

Financial support for this research is provided jointly by the Australian Research Council (Grant No. C00107787), the University of Technology, Sydney, Australia and Ion Automotive Systems, Sydney, Australia.

References

- [1] J.-S. Wu, C.-H. Chen, Torsional vibration analysis of gear-branched systems by finite element method, *Journal of Sound and Vibration* 240 (1) (2001) 159–182.
- [2] Ph. Couderc, J. Callenaere, J. Der Hagopian, G. Ferraris, Vehicle driveline dynamic behaviour: experiment and simulation, *Journal of Sound and Vibration* 218 (1) (1998) 133–157.
- [3] A. Crowther, N. Zhang, D.K. Liu, J. Jeyakumaran, A finite element method for dynamic analysis of automatic transmission gear shifting, *Proceedings of the Sixth International Conference on Motion and Vibration Control*, vol. 1, Saitama, Japan, 2000, pp. 514–519.
- [4] W. Reik, Torsional vibrations in the drive train of motor vehicles—principle considerations, in: *Proceedings of the Fourth International Symposium on Torsional Vibrations in the Drivetrain*, Baden-Baden, Germany, 20 April, 1990.
- [5] Torsional Analysis of BTR-Ford Vehicle Drive System, Borg Warner Automotive Transmission and Engine Components Corporation, Michigan. 13 October 1995.
- [6] M. Tsangarides, W. Tobler, Dynamic behaviour of a torque converter with centrifugal bypass clutch, SAE Technical Paper 850461, 1985.
- [7] S.-J. Hwang, J.-S. Chen, L. Liu, C.-C. Ling, Modeling and simulation of a powertrain vehicle system with automatic transmission, *International Journal of Vehicle Design* 23 (1) (2000) 145–160.
- [8] A. Farshidianfar, A. Ebrahimi, H. Bartlett, Hybrid modelling and simulation of the torsional vibration of driveline systems, *Proceedings of the Institution of Mechanical Engineers Part D: Journal of Automobile Engineering* 215 (1999) 217–229.
- [9] H. Kani, J. Miyake, T. Ninomiya, Analysis of the friction surface on clutch judder, *Japan Society of Automotive Engineers Review, Technical Notes* 12 (1) (1992) 82–84.
- [10] H.J. Drexl, Clutch judder—causes and countermeasures, in: *Proceedings of the Fourth International Symposium on Torsional Vibrations in the Drive Train*, Baden-Baden, Germany, 20 April 1990, pp. 109–124.
- [11] J.A.C. Martins, J.T. Oden, F.M.F. Simoes, Recent advances in engineering science—a study of static and kinetic friction, *International Journal of Engineering Science* 28 (1) (1990) 29–92.
- [12] B.R. Singh, Study of critical velocity of stick–slip sliding, *Journal of Engineering of Industry* (1960) 393–398.
- [13] B. Wiekil, B.J.M. Hill, Stick–slip motion for two coupled masses with side friction, *International Journal of Non-Linear Mechanics* 35 (2000) 953–962.
- [14] F. Van De Velde, P. De Bates, Mathematical approach of the influencing factors on stick–slip induced by decelerative motion, *Wear* 201 (1996) 80–93.
- [15] A. Crowther, N. Zhang, D. Liu, J.M. Jeyakumaran, Analysis and simulation of clutch engagement judder and stick–slip in automotive powertrain systems, *Proceedings of the Institution of Mechanical Engineers Part D: Journal of Automobile Engineering*, accepted for publication (2004).
- [16] H. Kohler, Gear dynamics—studies of ‘The State of the Art’, No. 2, British Gear Association Design Sub-Committee, December 1998.
- [17] M.T. Menday, H. Rahnejat, M. Ebrahimi, Clonk: an onomatopoeic response in torsional impact of automotive drivelines, *Proceedings of the Institution of Mechanical Engineers Part D: Journal of Automobile Engineering* 213 (1999) 349–357.
- [18] R. Krenz, Vehicle response to tip-in/tip-out, SAE Technical Paper 850967.
- [19] A. Fashindiar, Low frequency torsional vibration of vehicle drivelines in shuffle, in: H. Rahnejat (Ed.), *Multibody Dynamic Monitoring and Simulation Techniques*, 2000.
- [20] J.W. Biermann, B. Hagerodt, Investigation of the clonk phenomenon in vehicle transmissions—measurement, modeling and simulation, *Proceedings of the Institution of Mechanical Engineers Part K: Journal of Multibody Dynamics* 213 (1999) 53–60.
- [21] N. Zhang, A. Crowther, D.K. Liu, J. Jeyakumaran, A finite element method for the dynamic analysis of automatic transmission gear shifting with a 4DOF planetary gearset element, *Proceedings of the Institution of Mechanical Engineers Part D: Journal of Automobile Engineering* 217 (2003) 461–473.